

Supplementary Information

An ultra-low frictional interface combining FDTS SAMs with molybdenum disulfide

Xing'an Cao, Xuehui Gan, Yitian Peng*, Yongxia Wang, Xingzhong Zeng, Haojie Lang, Jinan Deng, Kun Zou

College of Mechanical engineering, Donghua University, Shanghai 201620, China

As shown in Figure S1, the surface of SiO₂ substrate appears to be flat and clean. The surface of FDTS SAMs-coated SiO₂ substrate reveals uniform islands. The XPS spectra of bare SiO₂ and FDTS SAMs are presented in Fig. S1. This spectra indicates the main elements including O_{1s}, Si_{2s}, Si_{2p} on the SiO₂ surface. The peaks corresponding to O_{1s}, C_{1s}, F_{1s} are observed on FDTS SAMs. FDTS SAMs have better capabilities of reducing the formation of capillary bridge. The reference value of thickness for the FDTS SAMs was 1.74 nm for perfluorodecyltrichlorosilane (FDTS) in ref. S5, which is close to 1.8 nm that was measured using an ellipsometer in ref. S6.

*Corresponding author. E-mail address: yitianpeng@dhu.edu.cn (Y.T. Peng).

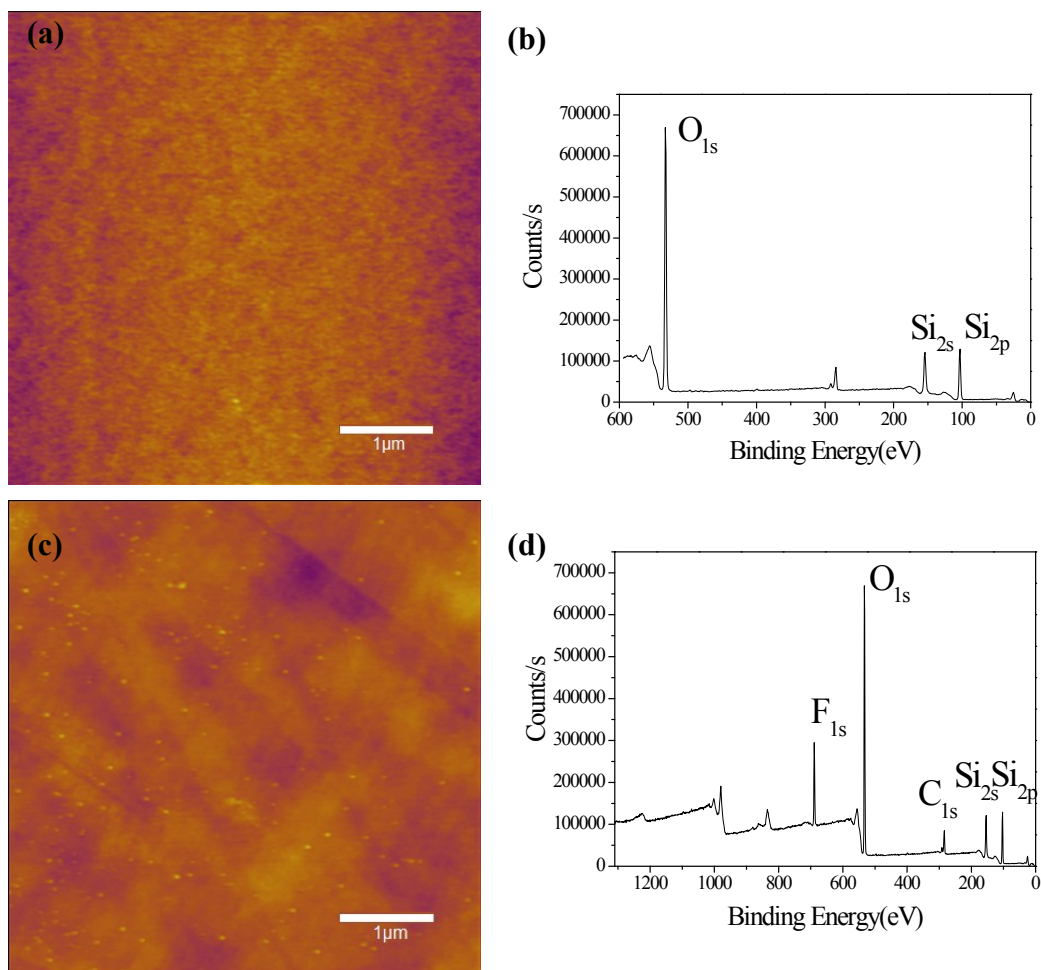


Figure S1. Topography and XPS spectra of Si/SiO₂ substrate(a,b) and FDTS SAMs deposited on Si/SiO₂ substrate(c,d)

Figure S2(a) shows optical microscopy image of MoS₂ nanosheets. Topographic image obtained under the tapping mode of AFM is shown in Figure S2(b). The thickness of MoS₂ nanosheets is about 3.1nm from the cross-sectional height profile(shown in Figure S2(d)). As shown in Figure S2(c), two characteristic Raman active modes for mechanically exfoliated MoS₂- E_{2g}^1 383 cm⁻¹ and A_{1g} 409 cm⁻¹—are present in the spectrum. These vibrational modes have been theoretically and experimentally investigated in bulk MoS₂²¹.

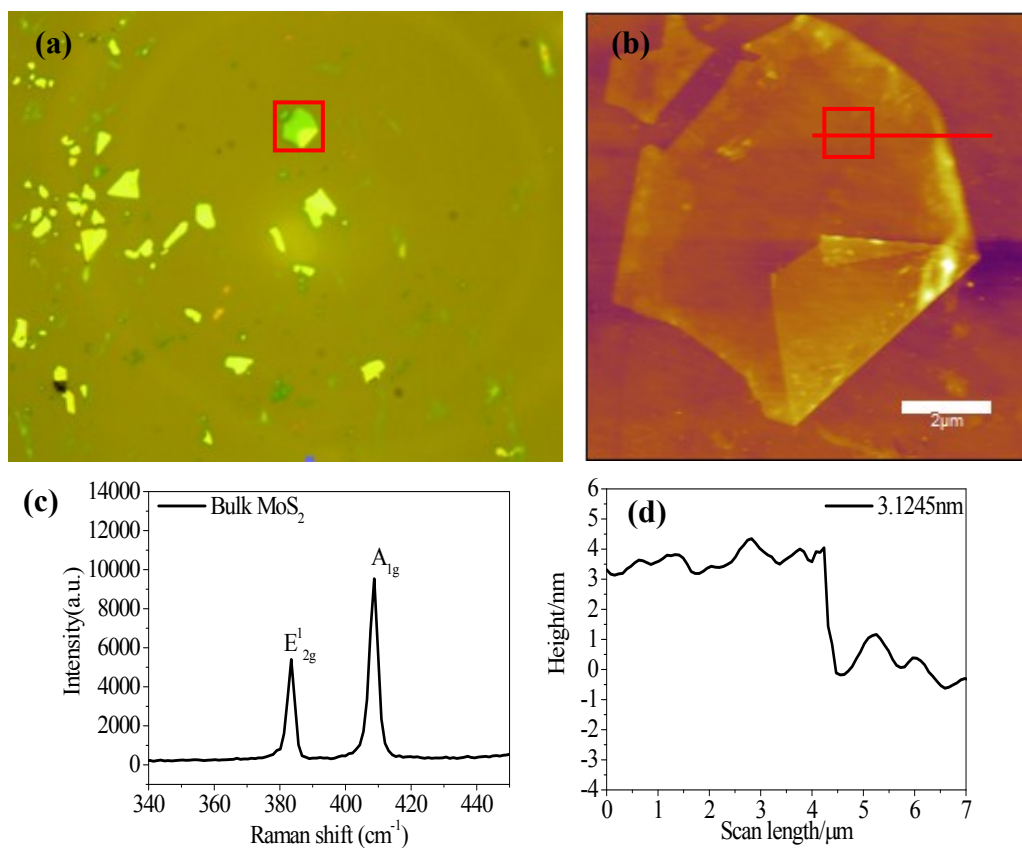


Figure S2. (a) Optical microscopy image, (b) AFM topographic image with (d) cross-sectional height profile below, and (c) Raman spectra of multi layer MoS₂ nanosheets. The red solid box in (a) is the location of topography imaging. The green solid line in (b) represents the cross-sectional profile

It is well known that WCA is related to the interfacial energy of solid surfaces through the Young's equation²⁴:

$$\gamma_{sv} = \gamma_{lv} \cos \theta + \gamma_{sl},$$

where γ_{sv} , γ_{lv} , γ_{sl} represent the solid surface free energy, liquid surface free energy, and solid-liquid interfacial energy respectively²⁵. θ is the WCA between the solid surface and liquid. Referring to the value of $\gamma_{lv} = 72.7 \text{ mJ/m}^2$ and the WCAs measured above^{26,27,28} (Table S1), the calculated surface energy of SiO₂, FDTS SAMs and MoS₂ were indicated. The surface energy was calculated by using Young's equation and referring to other's literature. The liquid-vapor interfacial energy of water was about

72.7mJ/m².

As for SiO₂, the values of water contact angle and total surface energy were 48.4° and 44.68 mN·m⁻¹(mJ/m²) in ref.26. The measured contact angle result of Si/SiO₂ in our experiment was 30.6°. Then we obtained that the calculated surface energy of Si/SiO₂ was about 58.99mJ/m².

For FDTs SAMs, the reference values of water contact angle and total surface energy were 115.4° and 9.95mJ/m²(see ref.27), respectively. Our experimental WCA of FDTs SAMs was 117.4°. The deduced solid-liquid interfacial energy was about 41.134mJ/m². The calculated surface energy of FDTs SAMs was about 7.68mJ/m².

For MoS₂, the reference surface energy and total contact angle of MoS₂ were 34.87mJ/m² and 89.9°(see ref.26). By the Young's equation and measured WCA value of 96.2°, The calculated SE value of MoS₂ was 26.89mJ/m². In consequence, the surface energy follows that $\gamma(\text{SiO}_2) > \gamma(\text{MoS}_2) > \gamma(\text{FDTs})$.

Table S1: Data obtained from wetting measurements and calculated work of adhesion of Si/SiO₂, FDTs SAMs and MoS₂.

Sample	water contact angle(degree)	surface energy (mJ/m ²)	work of adhesion (mJ/m ²)
Si/SiO ₂	30.6	58.99	135.3
FDTs SAMs	117.4	7.68	39.2
MoS ₂ on Si/SiO ₂	96.2	26.89	64.8

Table S1 shows the measured water contact angles(WCAs) of Si/SiO₂ substrate and FDTs SAMs. Figure S3 shows the images of a water droplet on the surfaces of SiO₂ substrate and the alkylsilane molecular films. Water contact angle values for Si/SiO₂ substrate, FDTs and MoS₂ are 30.6°, 117.4° and 96.2° respectively. Clearly, Si/SiO₂ substrate is relatively hydrophilic and alkylsilane monolayers are extremely hydrophobic since their WCAs exceed 90°. In fact, naturally defect-free MoS₂

nanosheets should be hydrophobic. The reason for the larger water WCA is assumed to be that the functional group $-CF_3$ in FDTS has a relatively lower surface tension than Si/SiO_2 substrate and MoS_2 .

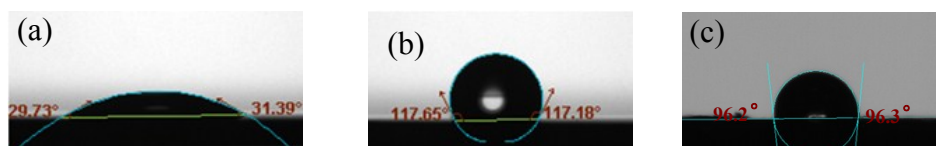


Figure S3. Water contact angles obtained on (a) Si/SiO_2 , (b)FDTS SAMs and (c) MoS_2

In general, the adhesive force consists of physical interaction such as van der Waals, electrostatic and capillary forces, and of chemical bonding such as hydrogen bonding. Under atmospheric environment, the electrostatic force and chemical bonding are usually considered to be neglected. Thereby the adhesive force between the tip and the sample is mainly determined by the meniscus force and the van der Waals force in the ambient condition²³. The meniscus force F_m is given as ²³

$$F_m = 2\pi R\gamma_l(\cos\theta_1 + \cos\theta_2) \quad (1)$$

where R is the asperity radius (tip radius here), γ_l is the surface tension of liquid (water), and θ_1 and θ_2 are the contact angle of the liquid with the two surfaces in contact, respectively. From Table S1, the order of contact angle value is $\theta(\text{FDTS}) > \theta(\text{MoS}_2) > \theta(\text{SiO}_2)$. Simultaneously, the calculated cosine of WCAs follow that $\cos(\text{SiO}_2) > \cos(\text{MoS}_2) > \cos(\text{FDTS})$. From Equation(1), the meniscus force is closely related to the water contact angle. A larger contact angle results in a lower meniscus force and adhesive force vice versa. Therefore, the adhesion force controlled by meniscus force follows that $F(\text{SiO}_2) > F(\text{MoS}_2) > F(\text{FDTS})$.

References:

- S1. R. T. Sanderson, *Science* (New York, N.Y.), 1952, **116**, 41-42.
- S2. S. Bartell, *Journal of the American Chemical Society*, 1959, **81**, 3497-3498.
- S3. A. C. Bond and L. O. Brockway, *Journal of the American Chemical Society*, 1954, **76**, 3312-3316.
- S4. A. J. Downs, G. S. McGrady, E. A. Barnfield, D. W. H. Rankin, H. E. Robertson, J. E. Boggs and K. D. Dobbs, *Inorganic Chemistry*, 1989, **28**, 3286-3292.
- S5. B. Bhushan, G. Kulik, L. Barbieri and P. Hoffmann, *Journal of Vacuum Science & Technology B*, 2005, **23**, 995-1003.
- S6. J. Choi, H. Morishita and T. Kato, *Applied Surface Science*, 2004, **228**, 191-200.